Fluid Dynamics & Materials Processing

Tech Science Press

Doi:10.32604/fdmp.2025.060255

ARTICLE

Experimental Investigation into the Impact of a Viscosity Reducer on the Crude Oil Recovery Rate in a Low-Permeability Reservoir

Baoyu Chen[1,2], Meina Li[3], Jicheng Zhang[1], Wenguo Ma[1,*], Yueqi Wang[1], Tianchen Pan[1] and Xuan Liu[1]

[1]Key Laboratory for Enhanced Oil and Gas Recovery of the Ministry of Education, Northeast Petroleum University, Daqing, 163318, China

[2]Daqing Oil Field Co. Ltd., Daqing, 163453, China

[3]The Second Working Area of the First Oil Production Plant, Daqing Oil Field Co. Ltd., Daqing, 163001, China

*Corresponding Author: Wenguo Ma. Email: mawenguo@nepu.edu.cn

Received: 28 October 2024; Accepted: 25 February 2025; Published: 30 June 2025

ABSTRACT: The relative permeability of oil and water is a key factor in assessing the production performance of a reservoir. This study analyzed the impact of injecting a viscosity reducer solution into low-viscosity crude oil to enhance fluid flow within a low-permeability reservoir. At 72°C, the oil-water dispersion solution achieved a viscosity reduction rate (f) of 92.42%, formulated with a viscosity reducer agent concentration (C_{VR}) of 0.1% and an oil-water ratio of 5:5. The interfacial tension between the viscosity reducer solution and the crude oil remained stable at approximately 1.0 mN/m across different concentrations, with the minimum value of 4.07×10^{-1} mN/m recorded at a C_{VR} of 0.2%. As the C_{VR} increased, the relative permeability curve of the oil phase gradually decreased while the oil-water two-phase region ($R_{o\text{-}wtp}$) expanded significantly. At a C_{VR} of 0.1%, the $R_{o\text{-}wtp}$ peaked, making an increase of 7.93 percentage points compared to water flooding. In addition, the final displacement efficiency ($E_{R,\,final}$) achieved with a 0.1% viscosity reducer solution reached 48.64%, exceeding water flooding by 15.46 percentage points, highlighting the effectiveness of the viscosity reducer solution in enhancing oil recovery.

KEYWORDS: Low-permeability reservoir; low-viscosity crude oil; viscosity reducer; relative permeability; oil displacement efficiency

1 Introduction

The growing global demand for petroleum products has driven a notable shift toward extracting unconventional crude oil. Low-permeability reservoirs account for 60%–70% of new oil and gas resources, making their development vital for global energy security [1,2]. These reservoirs exhibit challenging physical properties and complex pore structures. Zhang et al. categorized the oil and water dual-phase flow in these reservoirs as non-Darcy flow. Significant seepage resistance during flooding operations prevents the efficient transmission of pressure within the reservoir [3–5]. Water flooding is a commonly used method for developing low-permeability reservoirs and improving oil recovery performance. Oil and water seepage in these reservoirs exhibits non-Darcian behavior. Understanding the relative permeability of oil and water is crucial for characterizing seepage properties and predicting productivity [6,7]. The relative permeability of oil and water is influenced by several factors, including pore structure, wettability, fluid properties, interfacial tension, and displacement velocity, many of which are often uncontrollable in low-permeability reservoirs [8,9]. Low-viscosity crude oil in reservoirs experiences limited fluid flow. Therefore, it is vital to

develop a method for viscosity reduction that is both efficient and energy-saving. Current viscosity reduction methods include thermal recovery [10,11], oil dilution [12,13], emulsification [14], microbial methods [15,16], catalytic modification [17], and the use of viscosity reducers [18,19]. Chen et al. synthesized a side-chain functionalized copolymer (APVR) that penetrates the molecular structures of heavy oil. This process weakens the intermolecular forces between the heavy components by forming supramolecular interactions with the asphaltene. As a result, the asphaltene aggregates loosen, allowing the APVR's amphiphilic properties to aid in the emulsification of the oil droplets [20]. Currently, most viscosity reducer agents are mainly used for high-viscosity oils [21–23].

This study focuses on a crude oil reservoir in the target block, where the oil viscosity exceeds that of conventional crude oil but remains below the established threshold for heavy oil classification. The seepage behavior of the oil-water two-phase flow in low-viscosity crude oil reservoirs is not fully understood. Consequently, there is a pressing need to study the two-phase seepage patterns influenced by the viscosity reducer solutions on the crude oil viscosity. This study analyzes the changes in the fluid flow behavior within a low-permeability reservoir after injecting a viscosity reducer solution into low-viscosity crude oil.

2 Material and Methods

2.1 Material

2.1.1 Brine

The experiment used two types of water: simulated brine and treated oilfield wastewater. The simulated brine was prepared with a salinity of 6054.99 mg/L, reflecting the ionic composition of the reservoir water (Table 1). The viscosity measurement of the simulated brine at 72°C yielded 0.30 mPa·s. This simulated brine replaces the reservoir water in the flow experiment and the salt resistance analysis. The treated oilfield wastewater, the second fluid type employed in this study, was used to prepare the viscosity reducer solution. This solution was evaluated in the salt tolerance, interfacial tension, flowability, and oil displacement experiments. The viscosity of the treated oilfield wastewater was 0.35 mPa·s at 72°C. The viscosity data for both types of water at 72°C is shown in Table 2.

Table 1: Ionic components of the reservoir water

Anion (mg/L)				Cation (mg/L)			Total salinity (mg/L)	PH	Water type
HCO_3^-	CO_3^{2-}	Cl^-	SO_4^{2-}	K^++Na^+	Mg^{2+}	Ca^{2+}	6054.99	6.5	$CaCl_2$
183.06	0	3367.75	204.13	215.43	21.27	2063.35			

Table 2: Viscosity data of water at various temperatures

Temperature (°C)		35	45	55	65	75
Viscosity (mPa·s)	The simulated brine	1.10	0.80	0.65	0.40	0.30
	The treated oilfield wastewater	0.85	0.60	0.45	0.35	0.25

2.1.2 Crude Oil

Table 3 provides the viscosity measurements of the degassed crude oil from the Daqing oilfield over a temperature range of 50.0°C–75.0°C. The viscosity of the treated crude oil used in the interfacial tension and viscosity reduction rate tests was measured as 26.4 mPa·s at 72°C. A simulated oil, prepared by mixing kerosene and crude oil, demonstrated a viscosity of 18.0 mPa·s at 72°C. This simulated oil was used in both the oil-water relative permeability and oil displacement experiments.

Table 3: Viscosity measurements of the degassed crude oil at different temperatures

Temperature (°C)	**50**	**55**	**60**	**65**	**70**	**75**	**72**
Viscosity (mPa·s)	51.5	46.7	37.8	31.6	28.8	22.0	26.4

2.1.3 Viscosity Reducer High-Temperature Stability

The viscosity reducer solutions for the high-temperature stability experiments were prepared by mixing the treated oilfield wastewater with the viscosity reducer agents. The viscosity of the solution with a 0.3% C_{VR} was measured at 72.0°C. Fig. 1 shows the viscosity information of the solutions over time. The results show a slight increase in the viscosity of the solution when maintained at 72.0°C (the reservoir temperature) for 60 days.

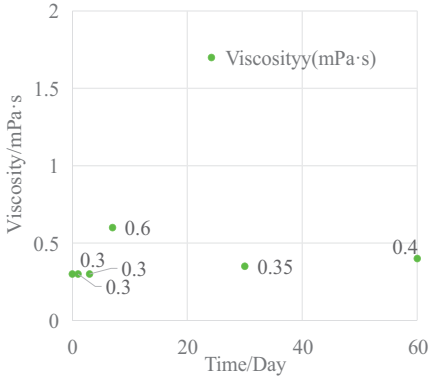

Figure 1: Viscosity stability results of the viscosity reducer solution at 72°C

2.1.4 The Salt Resistance Test

For the salt resistance experiments, the viscosity reducer solution was produced using the treated oilfield wastewater and the viscosity reducer agent with a C_{VR} of 0.3%. The salt resistance test solution was prepared by mixing the viscosity reducer (0.3% C_{VR}) and simulated brine (salinity 6054.99 mg/L) in a 1:1 volume ratio. The viscosity of the salt resistance test solution was measured at 72°C over different time intervals, as shown in Fig. 2. The salt resistance test solution maintained a constant viscosity, which demonstrates the good salt resistance of the viscosity reducer agent.

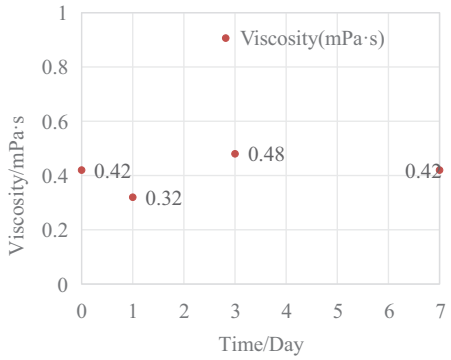

Figure 2: Viscosity of the salt-resistant test solution at 72.0°C

2.2 Methods

2.2.1 Viscosity Reduction Rate Test

Viscosity measurements of the effect of the viscosity reducer solution on low-viscosity crude oil were conducted using a Brookfield DV-II+Pro rotary viscometer, under the China Petroleum and Chemical Corporation Standard (Standard No. Q/SH 65-2013) [24]. Oil-water dispersion solutions with different oil-water ratios were prepared at 72°C using the viscosity reducer solution and simulated oil, which exhibited a viscosity of 18.0 mPa·s at the same temperature. The injection of the viscosity reducer solution into the original reservoir, before the start of water flooding, resulted in the preservation of a high original oil saturation within the reservoir. The viscosity reduction rate test employed oil-water dispersion solutions with oil-to-water ratios exceeding 1:1, which included 5:5, 7:3, 8:2, and 9:1. The viscosity reducer solution used to prepare the oil-water dispersion solutions had C_{VRs} of 0.05%, 0.1%, 0.15%, 0.2%, 0.25%, and 0.5%. The viscosity reduction rate of the oil-water dispersion solutions was evaluated.

The formula used to calculate the viscosity reduction rate (f) is as follows:

$$f = \frac{\mu_0 - \mu}{\mu_0} \tag{1}$$

where f represents the viscosity reduction rate as a percentage, μ_0 is the viscosity of the crude oil in mPa·s, and μ indicates the viscosity of the oil-water dispersion solution in mPa·s.

2.2.2 Oil-Water Relative Permeability

The oil-water relative permeability of the low-viscosity crude oil was determined using the unsteady state method, in compliance with the National Standard of the People's Republic of China (Standard No. GBT28912-2012) [25]. The core was first saturated with simulated brine before starting the oil-water relative permeability experiment. Subsequently, oil is injected at a steady rate until water production stops at the outlet. The injection pressure is monitored, and the original oil saturation (S_{oi}) and the bound water saturation (S_{wi}) are calculated.

The water injection rate was kept constant throughout the oil-water relative permeability experiment. As water production begins at the production end, the cumulative oil production, total liquid production, and displacement pressure difference are carefully recorded. During the early stages of water production, the time interval for recording should be minimized. Records are taken at regular intervals, including oil output periods. As the cumulative oil production decreases, the recording time interval is extended. Once the outlet water content reached 99.95%, the experiment tested the water phase permeability in the presence of residual

oil. The material balance method is employed to compute the bound water saturation (S_{ws}), corresponding water saturation (S_{we}), and relative permeability (K_{rw}, K_{ro}) at the end of the experiment, considering the final water content (f_w).

$$f_o\left(S_{\mathrm{w}}\right)=\frac{\mathrm{d}\overline{V}_{\mathrm{o}}\left(t\right)}{\mathrm{d}\overline{V}\left(t\right)} \tag{2}$$

$$K_{\mathrm{ro}}=f_{\mathrm{o}}\left(S_{\mathrm{w}}\right)\frac{\mathrm{d}\left[1/\overline{V}\left(t\right)\right]}{\mathrm{d}\left[1/I\overline{V}\left(t\right)\right]} \tag{3}$$

$$K_{\mathrm{rw}}=K_{\mathrm{ro}}\frac{\mu_{\mathrm{w}}}{\mu_{\mathrm{o}}}\frac{1-f_{\mathrm{o}}\left(S_{\mathrm{w}}\right)}{f_{\mathrm{o}}\left(S_{\mathrm{w}}\right)} \tag{4}$$

$$I=\frac{Q\left(t\right)}{Q_0}\frac{\Delta p_{\mathrm{o}}}{\Delta p\left(t\right)} \tag{5}$$

$$S_{\mathrm{we}}=S_{\mathrm{ws}}+\overline{V}_{\mathrm{o}}\left(t\right)-\overline{V}\left(t\right)f_{\mathrm{o}}\left(S_{\mathrm{w}}\right) \tag{6}$$

where $f_{\mathrm{o}}(S_w)$ represents the oil content value expressed as a decimal; the dimensionless cumulative oil production, $\overline{V}_{\mathrm{o}}\left(t\right)$ is given as a multiple of pore volume; the dimensionless cumulative fluid recovery $\overline{V}\left(t\right)$ is also expressed as a multiple of the pore volume; the relative injection capacity (I), also known as the flow capacity ratio, is provided; the relative permeability value of the water phase K_{rw} is expressed as a decimal; K_{ro} denotes the relative permeability value of the oil phase is similarly expressed as a decimal; $Q(t)$ represents the liquid production flow value at the outlet end face of the rock sample at time t, measured in cubic centimeters per second (cm^3/s); Q_{o} is the oil production flow value at the outlet end face of the rock sample at the initial time, in cubic centimeters per second (cm^3/s); the initial drive pressure difference ΔP_{o} expressed in MPa; $\Delta P(t)$ denotes the displacement pressure difference at time t; S_{we} indicates the water saturation value on the end face of the outlet of the rock sample, expressed as a decimal; f_w is the water content, and %; S_{ws} represents the bound water saturation, expressed as a percentage (%).

3 Effect of the Crude Oil Performance Test on the Viscosity Reducer Solution

3.1 Effect of the Viscosity Reducer Agent Concentration on the Viscosity Reduction Rate

Oil-water dispersion solutions with oil-to-water ratios of 5:5, 7:3, 8:2, and 9:1 were prepared at 72°C by combining the viscosity reducer solution with the treated crude oil, which has a viscosity of 26.4 mPa·s at the same temperature. The C_{VR} of the oil-water dispersion solution was set at 0.05%, 0.1%, 0.15%, 0.2%, 0.25%, and 0.5% for each oil-to-water ratio. The viscosities and viscosity reduction rates obtained are shown in Table 4 and Fig. 3.

Table 4: The viscosity and f of the oil-water dispersion solution with varying C_{VR} under different oil-to-water ratios

C_{VR} (%)	Oil-water ratio							
	5:5		7:3		8:2		9:1	
	Viscosity (mPa·s)	f (%)	Viscosity (mPa·s)	f (%)	Viscosity (mPa·s)	f (%)	Viscosity (mPa·s)	f (%)
0.00	35.2	−75.74	35.6	−34.85	37.8	−43.18	36.3	−37.50
0.05	3.7	85.98	32.7	−23.86	37.20	−40.91	31.8	−20.45
0.10	2.0	92.42	30.4	−15.15	37.4	−41.67	29.4	−11.36
0.15	4.1	84.47	29.7	−12.50	37.6	−42.42	30.7	−16.29

(Continued)

Table 4 (continued)

C_{VR} (%)	Oil-water ratio							
	5:5		7:3		8:2		9:1	
	Viscosity (mPa·s)	f (%)	Viscosity (mPa·s)	f (%)	Viscosity (mPa·s)	f (%)	Viscosity (mPa·s)	f (%)
0.20	4.5	82.95	27.9	−5.68	36.9	−39.77	32.1	−21.59
0.25	4.4	83.33	29.3	−10.98	37.6	−42.42	33.6	−27.27
0.50	8.2	68.94	35.6	−34.85	37.8	−43.18	36.3	−37.50

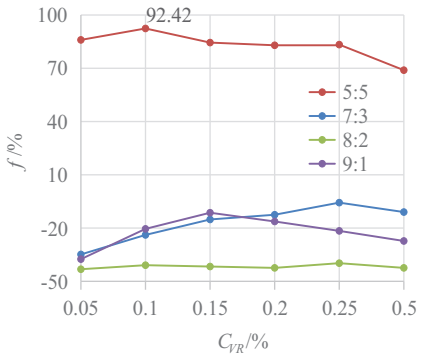

Figure 3: The f of the oil-water dispersion solution with different C_{VRs} under varying oil-to-water ratios

Table 4 and Fig. 3 present the experimental findings that highlight the impact of C_{VR} on the rate of viscosity reduction across different oil-water dispersion solutions. A maximum viscosity reduction rate of 92.42% was achieved in a 5:5 oil-water dispersion solution with a C_{VR} of 0.1%.

3.2 Effect of the Oil-Water Ratio on the Viscosity Reduction Rate

Oil-water dispersion solutions were prepared at 72°C using a viscosity reducer solution (C_{VR} of 0.1%) and the treated crude oil with a viscosity of 26.4 mPa·s at the same temperature, varying the oil-to-water ratios. Table 5 and Fig. 4 present the experimental results for the viscosity reduction rate.

Table 5: Viscosity of the oil-water dispersion solution with varying oil-water ratios (at C_{VR} = 0.1%)

Oil-water ratio	Viscosity (mPa·s)	f (%)
10:0	26.4 (crude oil)	0.0
9:1	31.8	−20.45
8:2	37.2	−40.91
7:3	32.7	−23.86
6:4	14.7	44.32
5:5	2.0	92.42

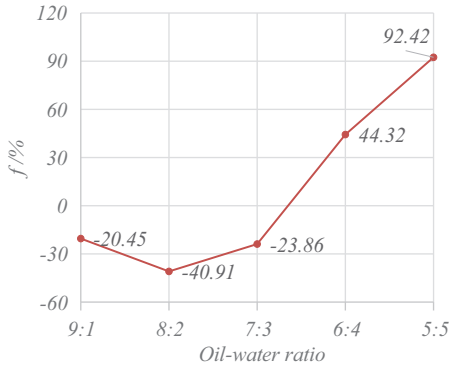

Figure 4: The f of the oil-water dispersion solution with different oil-to-water ratios (the C_{VR} = 0.1%)

When the oil-to-water ratio ranges from 9:1 to 7:3, the viscosity of the oil-water dispersion solution exceeds that of the treated crude oil. As the oil-to-water ratio transitions from 6:4 to 5:5, the viscosity of the oil-water dispersion solution decreases, enhancing the effectiveness of the viscosity reduction agent.

4 The Interfacial Tension Test

The interfacial tension between the viscosity reducer solution and the crude oil was measured experimentally at varying concentrations of the viscosity reducer solution, ranging from 0.0% to 1.0%. The interfacial tension stabilized for each C_{VR} after 80 min. Fig. 5 shows the variation in the interfacial tension over time. Fig. 6 displays the final stable interfacial tension values for various C_{VR}. The solution demonstrating a C_{VR} of 0.2% exhibited the minimum interfacial tension, measured at 4.07×10^{-1} mN/m. The interfacial tension data of the remaining solution were observed to be close to 1.0 mN/m.

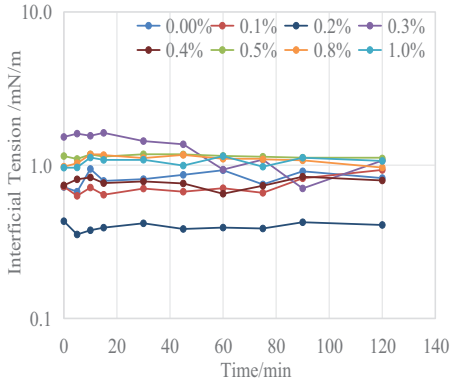

Figure 5: Interfacial tension at different intervals between the viscosity reducer solution (with varying C_{VR}) and the crude oil

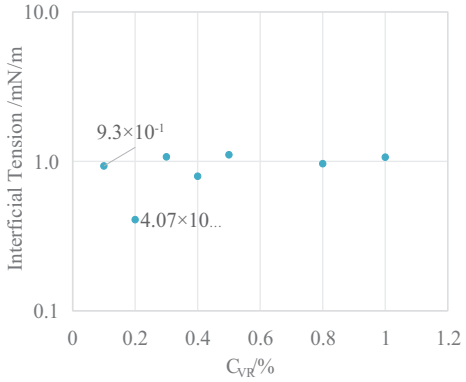

Figure 6: The final stable interfacial tension between the viscosity reducer solution and the crude oil at varying C_{VR}

5 Oil-Water Relative Permeability Experiments

5.1 Experimental Conditions

The simulated oil, created for testing by mixing kerosene and crude oil, displayed a viscosity of 18.0 mPa·s at 72°C, which matches the crude oil viscosity under the reservoir conditions. Table 6 presents the relative permeability curve obtained using the unsteady state method and the natural core parameters.

Table 6: Natural core parameter

Core number	Core length (cm)	Diameter (cm)	K_g ($\times10^{-3}\mu m^2$)	K_w ($\times10^{-3}\mu m^2$)	Pore volume (cm^3)	Φ (%)
949-3	6.58	2.53	1.60	0.21	4.40	13.31
949-14	5.00	2.53	2.50	0.48	3.52	14.01

5.2 Results of the Oil-Water Relative Permeability Experiment

In the oil-water relative permeability experiments, an injection volume of 0.1 PV was used for the viscosity reducer solution. The C_{VR} of the solution was systematically varied across a range of values, specifically 0.0% to 5.0% (0.0%, 0.5%, 0.8%, 1.0%, 2.0%, and 5.0%). After the injection of the viscosity reducer solution slug, the water injection rate for the oil-water relative permeability experiment was kept constant at 0.05 mL/min. The results of these oil-water relative permeability experiments are shown in Table 7 and Fig. 7.

Table 7: Experimental data for the oil-water relative permeability of the natural core

C_{VR} (%)	Φ (%)	K_w ($\times10^{-3}\mu m^2$)	S_{oi} (%)	S_{ws} (%)	S_{or} (%)	$R_{o\text{-}wtp}$ (%)	$E_{R,\,final}$ (%)
0.00	13.31	0.21	57.95	42.05	39.32	18.58	32.16
0.05	14.01	0.48	57.67	42.33	36.36	21.23	36.95
0.08	13.34	0.20	56.67	43.33	33.32	23.25	41.20
0.10	13.45	0.48	57.40	42.60	30.77	26.51	46.39
0.20	12.79	0.21	57.92	42.08	32.62	24.76	43.67
0.50	13.25	0.48	57.06	42.94	33.03	23.09	42.11

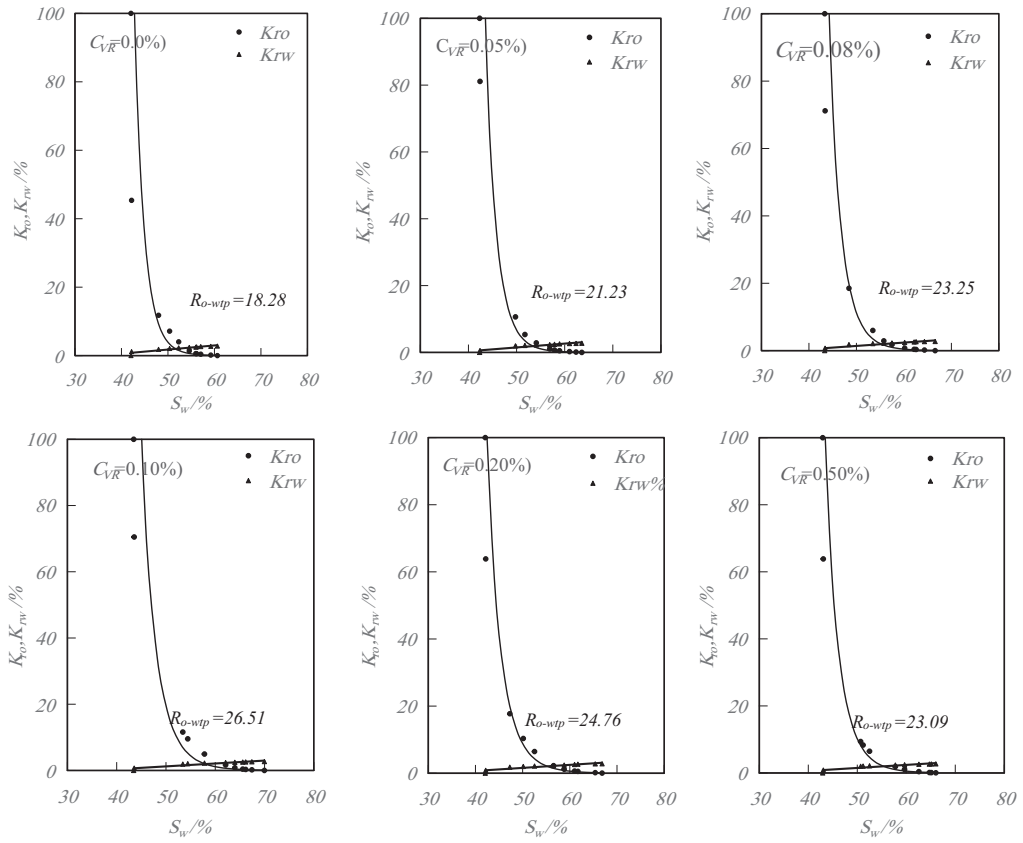

Figure 7: Oil-water relative permeability curves following the injection of the viscosity reducer solution at different C_{VR} values

A positive correlation was observed between the C_{VR} of the viscosity reducer solution and the decrease in oil phase relative permeability. Simultaneously, the gap between the two phases showed a widening trend. The oil-water two-phase flow ratio ($R_{o\text{-}wtp}$) peaked at a C_{VR} of 0.1%, showing an increase of 7.93 percentage points compared to water flooding.

6 Oil Displacement Experiment of the Viscosity Reducer Solutions

6.1 Experimental Conditions

For the oil displacement experiments, the simulated oil was formulated by blending kerosene and crude oil, yielding a viscosity of 18.0 mPa·s at 72°C. Table 8 lists the parameters of the natural core used in the oil displacement experiments.

Table 8: Natural core parameter

Core number	Core length (cm)	Diameter (cm)	K_g ($\times 10^{-3}$ μm^2)	K_w ($\times 10^{-3}$ μm^2)	Pore volume (cm^3)	Φ (%)
109-13	5.00	2.53	3.6	0.65	3.81	15.18
109-15	5.00	2.53	3.0	0.60	3.73	14.86

6.2 Experimental Results and Analysis

An experiment was performed to assess the oil displacement effectiveness ($E_{R,\ final}$) of a viscosity reducer solution. In this experiment, 0.1 PV of the solution was injected before initiating water flooding. In each scheme, the C_{VR} of the viscosity reducer was systematically varied, assuming values of 0.00%, 0.05%, 0.08%, 0.10%, 0.20%, and 0.50%, respectively. Next, water flooding was carried out at a rate of 0.05 mL/min. The results of this experiment are shown in Table 9 and Fig. 8.

Table 9: Experimental results of natural core oil displacement

C_{VR} (%)	Φ (%)	K_w ($\times 10^{-3}\mu m^2$)	S_{oi} (%)	S_{ws} (%)	S_{or} (%)	$E_{R,\ final}$ (%)
0.00	15.17	0.65	57.74	42.26	38.58	33.18
0.05	14.81	0.60	59.14	40.86	37.10	37.27
0.08	14.85	0.64	58.98	41.02	34.05	42.27
0.10	14.93	0.60	58.67	41.33	30.13	48.64
0.20	15.48	0.65	56.56	43.44	32.13	43.18
0.50	14.85	0.60	58.98	41.02	34.32	41.82

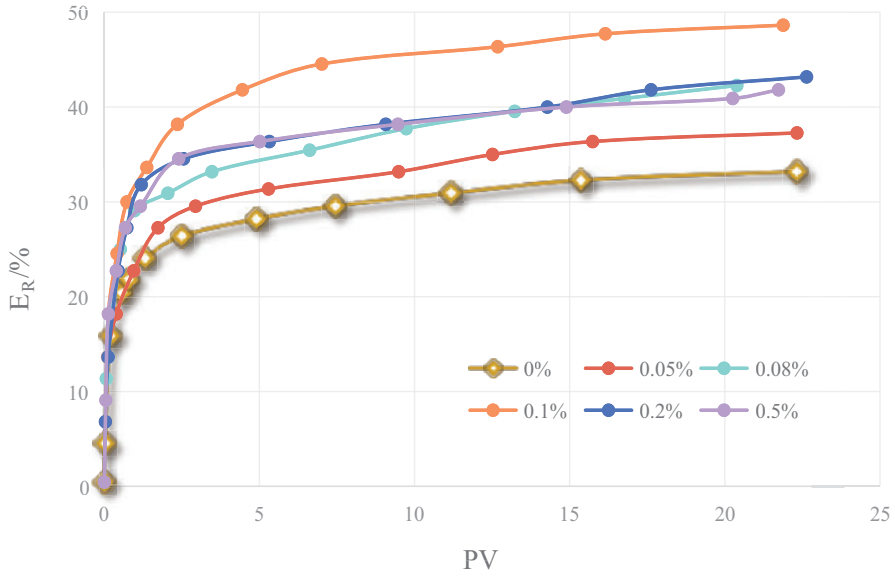

Figure 8: Oil displacement efficiency curves with different C_{VR} values

The final oil recovery efficient $E_{R,\ final}$ attained by the viscosity reducer solution flooding at a C_{VR} of 0.1% was 48.64%, exhibiting a 15.46 percentage point improvement over conventional water flooding.

6.3 Economic Benefit Analysis

The experimental well group within the research block is composed of one injection well and six production wells, as shown in Fig. 9. The oil layer has a thickness of 18.5 m, with a distance of 364 m separating the injection and production wells. The well group control area covers 0.28 km^2, with a formation pore

volume of 72.52 × 10^4 m^3 and geological reserves totaling 18.34 × 10^4 tons. All these data are presented in Table 10.

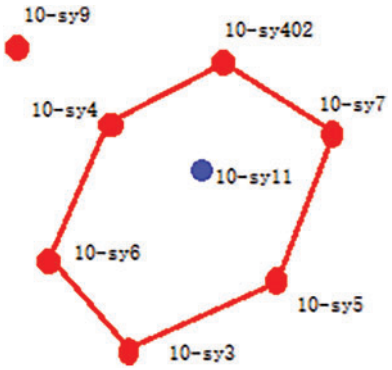

Figure 9: Location map of the test well group

Table 10: Experimental data on oil displacement in natural core

Pore volume/×10^4 m^3	Crude oil geological reserve/ ×10^4 ton	VR solution dosage/PV	C_{VR}/%	VR price /($/ton)	Input cost/×10^4 $	Oil increase/ ×10^4 ton	Crude oil price/$/ barrel	Income increase/ ×10^4 $	Benefit/ ×10^4 $
72.52	18.34	0.1	0.1	1000	7.252	2.835	73.28	1522.99	1515.738

The results of the laboratory oil displacement experiment show that the viscosity reducer solution flooding increased the oil recovery by 15.46 percentage points compared to water flooding. After implementing this scheme, the experimental well group is expected to produce an additional 2.83 × 10^4 tons of oil.

The viscosity reducer solution was injected at a volume of 0.1 PV and a C_{VR} of 0.1% wt. A total of 72.52 tons of the viscosity reducer agent was used in the test. The viscosity reducer agent was priced at US $1000 per ton, leading to a total input cost of US $72,252. With an oil increase ratio of 15.46%, the crude oil production increase for the well group's controlled reserves is 28,350 tons. At a crude oil price of US $73.28 per barrel, the income from oil production totals US $15,229,900. As a result, the profit increase from oil production following the injection of the viscosity reducer solution is US $15,157,380.

7 Conclusions

Laboratory investigations were performed to evaluate the influence of the viscosity reducer solutions on the performance of the low-viscosity crude oil. The experimental program included both oil-water relative permeability tests and oil displacement experiments conducted with low-viscosity crude oil.

(1) At 72°C, with an oil-to-water ratio of 5:5 and a C_{VR} of 0.1% in the oil-water dispersion solution, the viscosity reduction rate of the viscosity reducer solution reached 92.42%.

(2) The interfacial tension between the viscosity reducer solution and the crude oil remains relatively stable, staying close to 1.0 mN/m across various concentrations. The viscosity reducer solution at a C_{VR} of 0.2% demonstrates the minimum interfacial tension at 4.07 × 10^{-1} mN/m.

(3) A positive correlation exists between increasing C_{VR} and a gradual decrease in the oil phase relative permeability curve. Concurrently, the span between the two phases demonstrates a widening trend. The $R_{o\text{-}wtp}$ attains its peak at a C_{VR} of 0.1%, showing a 7.93% point increase compared to water flooding.

(4) The final efficiency ($E_{R,\,final}$) of the viscosity reducer solution flooding with a C_{VR} of 0.1%, reached 48.64%, representing a 15.46 percentage point increase over water flooding.

Acknowledgement: None.

Funding Statement: The research was supported by the Petrochina Daqing Oilfield Research Project (No. DQYT-1201002-2023-JS-1201).

Author Contributions: Investigation: Baoyu Chen, Meina Li; Resources: Meina Li, Jicheng Zhang; Funding acquisition: Baoyu Chen, Jicheng Zhang; Experiment: Wenguo Ma, Yueqi Wang, Tianchen Pan, Xuan Liu; Methodology: Baoyu Chen, Jicheng Zhang, Wenguo Ma; Data curation: Wenguo Ma, Yueqi Wang. All authors reviewed the results and approved the final version of the manuscript.

Availability of Data and Materials: The datasets generated or analyzed during the current study are available from the corresponding author on reasonable request.

Ethics Approval: Not applicable.

Conflicts of Interest: The authors declare no conflicts of interest to report regarding the present study.

References

1. Jia C, Wang Z, Jiang L. Achievements and future potential for oil & gas exploration and development in China: deep-formation, deep-water and unconventional reservoirs—interview with JIA Chengzao, Academician of the CAS, geologist in petroleum geology and structure. World Pet Indust. 2023;30(3):1–8.
2. Samara H, Ke L, Ostrowski T, Ganzer L, Jaeger P. Unconventional oil recovery from Al Sultani tight rock formations using supercritical CO_2. J Supercrit Fluids. 2019;152:104562.
3. Zhang WL. Technology of water injection development in ultra-low permeability reservoir. IOP Conf Ser: Earth Environ Sci. 2020;558(2):022001.
4. Liu JJ, Liu XG, Hu YR. Study on Nonlinear seepage of rock of low permeability. Chin J Rock Mech Eng. 2003;4:556–61.
5. Taborda EA, Franco CA, Lopera SH, Alvarado V, Cortés FB. Effect of nanoparticles/nanofluids on the rheology of heavy crude oil and its mobility on porous media at reservoir conditions. Fuel. 2016;184:222–32.
6. Torabi F, Mosavat N, Zarivnyy O. Predicting heavy oil/water relative permeability using modified Corey-based correlations. Fuel. 2016;163:196–204.
7. Zhang N, Yan B, Sun Q, Wang Y. Improving multi scale mixed finite element method for flow simulation in highly heterogeneous reservoir using adaptivity. J Pet Sci Eng. 2017;154:382–8.
8. Nguyen VH, Sheppard AP, Knackstedt MA, Pinczewski WV. The effect of displacement rate on imbibition relative permeability and residual saturation. J Pet Sci Eng. 2006;52:54–70.
9. Wang JX, Buckley JS. In wettability and rate effects on end-point relative permeability to water. In: Proceedings of the International Symposium of the Society of Core Analysts, Proceedings of the International Symposium of the Society of Core Analysts; 1999; Golden, CO, USA. p. 1–50.
10. Xue L, Liu PC, Zhang Y. Development and research status of heavy oil enhanced oil recovery. Geofluids. 2022;2022:1–30. doi:10.1155/2022/5015045.
11. Omoregbe O, Hart A. Global trends in heavy oil and bitumen recovery and *in-situ* upgrading: a bibliometric analysis during 1900–2020 and future outlook. ASME J Energy Resour Technol. 2022 Dec;144(12):123007. doi:10.1115/1.4054535.
12. Jing JQ, Yin R, Zhu G, Xue J, Wang S, Wang S. Viscosity and contact angle prediction of low water-containing heavy crude oil diluted with light oil. J Pet Sci Eng. 2019;176(7):1121–34. doi:10.1016/j.petrol.2019.02.012.

13. Dehaghani AHS, Badizad MH. Experimental study of Iranian heavy crude oil viscosity reduction by diluting with heptane, methanol, toluene, gas condensate and naphtha. Petroleum. 2016;2(4):415–24. doi:10.1016/j.petlm.2016.08.012.
14. de Farias MLR, Campos EF, de Souza ALS, Carvalho MS. Injection of dilute oil-in-water emulsion as an enhanced oil recovery method for heavy oil: 1D and 3D flow configurations. Transp Porous Media. 2016;113(2):267–81. doi:10.1007/s11242-016-0692-0.
15. Sakthipriya N, Doble M, Sangwai JS. Performance of thermophilic strain on the reduction of viscosity of crude oil under high pressure and high temperature conditions: experiments and modeling. J Pet Sci Eng. 2022;210:110016. doi:10.1016/j.petrol.2021.110016.
16. Lavania M, Cheema S, Lal B. Potential of viscosity reducing thermophillic anaerobic bacterial consortium TERIB#90 in upgrading heavy oil. Fuel. 2015;144(31):349–57. doi:10.1016/j.fuel.2014.12.003.
17. Clark PD, Hyne JB, Tyrer JD. Influence of PH on the high temperature hydrolysis of tetrahydrothiophene and thiophene. Fuel. 1984;63:125–8.
18. Anto R, Deshmukh S, Sanyal S, Bhui UK. Nanoparticles as flow improver of petroleum crudes: study on temperature-dependent steady-state and dynamic rheological behavior of crude oils. Fuel. 2020;275(5):117873. doi:10.1016/j.fuel.2020.117873.
19. Roland N, Andrea E, László B, Máté H, Sándor P. Study on the dynamic viscosity of crude oil-in-water emulsions. Pet Sci Technol. 2021;39(19–20):896–907. doi:10.1080/10916466.2021.1959610.
20. Chen M, Wang Y, Chen W, Ding M, Zhang Z, Zhang C et al. Synthesis and evaluation of multi-aromatic ring copolymer as viscosity reducer for enhancing heavy oil recovery. Chem Eng J. 2023;470:144220. doi:10.1016/j.cej.2023.144220.
21. Taghili N, Manteghian M, Jafari A. Novel preparation of MoO_3/γ-Al_2O_3 nanocatalyst: application in extra-heavy oil visbreaking at atmospheric pressure. Appl Nanosci. 2020;10(5):1–11.
22. Montes D, Henao J, Taborda EA, Gallego J, Cortés FB, Franco CA. Effect of textural properties and surface chemical nature of silica nanoparticles from different silicon sources on the viscosity reduction of heavy crude oil. ACS Omega. 2020;5(10):5085–97. doi:10.1021/acsomega.9b04041.
23. Hasan MM, Al-Zuhairi FK, Sadeq AH, Azeez RA. Assessment of nanoparticle-enriched solvents for oil recovery enhancement. Fluid Dyn Mater Process. 2023;19(11):2827–35. doi:10.32604/fdmp.2023.027746.
24. Xu Z, Li M, Kong Y, Long C, Sun Y, Liu G, et al. Synthesis and performance evaluation of graphene-based comb polymer viscosity reducer. Energies. 2023;16(15):5779. doi:10.3390/en16155779.
25. Zhang ZB, Luo ML, Dai ZJ. GB/T 28912-2012, test method for two phase relative permeability in rock, experimental ability in rock. Beijing, China: Petroleum Industry Press; 2012.